Non-Mechanical Two-Dimensional Optical Beam Deflector Operated by Wavelength Tuning

Morio Toyoshima*
Vienna University of Technology, Gusshausstrasse 25/389, A-1040 Wien, Austria

National Institute of Information and Communications Technology (NICT), 4-2-1 Nukui-Kitamachi, Koganei, Tokyo 184-8795, Japan

Franz Fidler†, Martin Pfennigbauer‡, and Walter R. Leeb§
Vienna University of Technology, Gusshausstrasse 25/389, A-1040 Wien, Austria

A new method based on an optical delay line structure is proposed for two-dimensional optical beam steering. For one-dimensional beam steering, the laser beam to be deflected is split into *N* co-directional sub-beams of equal intensity with the aid of a plane-parallel plate. These sub-beams experience a relative time delay, which translates into a phase difference, thus forming a phased array. When the laser wavelength is tuned, the relative phase varies and the far-field interference footprint can be steered across a receive plane. By employing two plane-parallel plates in series, the described scheme can be extended to produce a two-dimensional *N* × *N*, array of sub-beams, allowing two-dimensional beam steering via wavelength tuning. In this paper, preliminary experimental results with four sub-beams are presented.

Nomenclature

a	=	aperture spacing of two consecutive beams
α_x	=	deflection sensitivity coefficients for the x direction
α_y	=	deflection sensitivity coefficients for the y direction
d	=	thickness of first MBG device
d'	=	thickness of second MBG device
$\Delta\Phi_B$	=	optical phase difference at point B
$\Delta\Phi_C$	=	optical phase difference at point C
$\Delta\Phi$	=	optical phase difference between points B and C
f	=	focal length of a lens
γ	=	ratio of optical delay and aperture spacing
I	=	optical power of the input beam
i	=	number of i-th beams
I_i	=	optical power of the i-th output beam
η	=	transmission efficiency of the device
k_0	=	wave number before wavelength tuning
λ_0	=	wavelength before wavelength tuning
λ_1	=	wavelength after wavelength tuning
m	=	thickness scaling factor
N	=	total number of beams along one axis
n_1	=	refractive index of air
n_2	=	refractive index of optical glass

*Guest scientist, Institute of Communications and Radio-Frequency Engineering, Vienna University of Technology, and Senior Research Engineer, Wireless Communications Department, NICT.
†Doctoral student, Institute of Communications and Radio-Frequency Engineering.
‡Assistant professor, Institute of Communications and Radio-Frequency Engineering.
§Professor, Institute of Communications and Radio-Frequency Engineering.

Φ_B = optical phase at point B
Φ_C = optical phase at point C
R = mirror reflectance
R_i = beam splitter reflectance for the i-th beam
θ_{def} = deflection angle of the beam
θ_x = deflection angles for x direction
θ_y = deflection angles for y direction
θ_1 = angle of incidence
θ_2 = angle of refraction
x = x axis at the receive plane
y = y axis at the receive plane

I. Introduction

Optical free-space multiple access systems employing laser beams that connect optical transceivers offer new potential applications in laser communications.[1-4] It is expected that such a scheme will be used in satellite clusters, distributed satellite systems, and formation-flying satellites, or even in free-space optical switching applications.[5-7] Several methods of deflecting optical beams exist, and they are based on five techniques or devices: mechanical steering using mirrors, real-time re-writable holograms, liquid crystals, acousto-optic devices, or optical phased arrays.[1,8,9] The first three approaches are slow. Acousto-optic devices are fast, but they suffer from low efficiency and produce an unwanted zero-order diffraction beam. The "classical" optical phased array has a fast response but is quite complex, as it requires individual phase control of the optical sub-beams.[10,11]

We propose a new method based on an optical delay line structure. For one-dimensional beam steering, the laser beam to be deflected is split into N co-directional sub-beams of equal intensity with the aid of a plane-parallel plate. These sub-beams experience a relative time delay, which translates into a phase difference, thus forming a phased array. When the laser wavelength is tuned, the relative phases vary and, as a consequence, the far-field interference footprint is steered across the receive plane. Beam steering can be very fast, limited only by the rate of laser wavelength tuning. However, according to recent results, optical frequency modulation techniques[12,13] can modulate laser wavelengths at rates of several gigahertz.

This paper presents preliminary experimental results for a plane-parallel plate, named the multiple beam generator (MBG), with four sub-beams. The next section describes the principle of the beam deflection, with the optical wavelength as the main independent variable. By employing two plane-parallel plates in series, the scheme can be extended to produce a two-dimensional $N \times N$, array of sub-beams, allowing two-dimensional beam steering via wavelength tuning. Section 3 describes the experimental setups for the one- and two- dimensional beam scanning and presents the measurement results. The effect of random phase error of the sub-beams is evaluated and the phase difference is checked using an interferometric setup in Section 4.

II. Principle of the beam deflection

A. Equal intensity multibeam generation

The MBG device basically consists of two optical surfaces, namely a beam splitter and a mirror. These two surfaces enable us to realize an optical delay line and generate parallel beams. The geometry of the optical delay line for the MBG is shown in Fig. 1 (In Fig. 1 the beam enters the device from the left through an anti-refection coating). The incident light passes through the beam splitter surface with reflectance R_1 so that an output beam becomes available at point A. The light reflected by the beam splitter is then reflected by the mirror surface, and a second output beam is transmitted parallel to the first one at point C. In a similar manner, the i-th beam is reflected by a beam splitter with reflectance R_i. The reflectance R_i on the beam splitter surface at the i-th beam is chosen as[14]

$$R_i = 1 - \frac{1}{N-(i-1)}, \tag{1}$$

where N is the total number of beams on one axis.

B. Optical phase difference

We refer to Fig. 1 to calculate the optical phase difference (OPD) between two consecutive output beams in an output plane normal to the output beam direction. For distances $\overline{AB}$ and $\overline{ADC}$, we obtain

$$\overline{AB} = 2d \tan\theta_2 \sin\theta_1 = \frac{2n_2 d \sin^2\theta_2}{n_1 \cos\theta_2}, \tag{2}$$

$$\overline{ADC} = 2\overline{AD} = \frac{2d}{\cos\theta_2}, \tag{3}$$

where $n_1 \sin\theta_1 = n_2 \sin\theta_2$. With θ_1 and θ_2, we denote the incident and refractive angles of the beam, where n_1 and n_2 are the refractive indices of the media. The optical phases Φ_B and Φ_C at points B and C relative to that at point A are given by

$$\Phi_B = k_0 \cdot \overline{AB} = \frac{2\pi}{\lambda_0} \frac{2n_2 d \sin^2\theta_2}{n_1 \cos\theta_2}, \tag{4}$$

$$\Phi_C = n_2 k_0 \cdot \overline{ADC} = \frac{2\pi}{\lambda_0} \frac{2n_2 d}{\cos\theta_2}, \tag{5}$$

where k_0 is the wave number ($=2\pi/\lambda_0$), λ_0 the vacuum wavelength, and d the thickness of the MBG. When the wavelength is changed to λ_1, the phase at points B and C change by

$$\Delta\Phi_B = \frac{2n_2 d \sin^2\theta_2}{n_1 \cos\theta_2} \left(\frac{2\pi}{\lambda_1} - \frac{2\pi}{\lambda_0} \right), \tag{6}$$

$$\Delta\Phi_C = \frac{2n_2 d}{\cos\theta_2} \left(\frac{2\pi}{\lambda_1} - \frac{2\pi}{\lambda_0} \right), \tag{7}$$

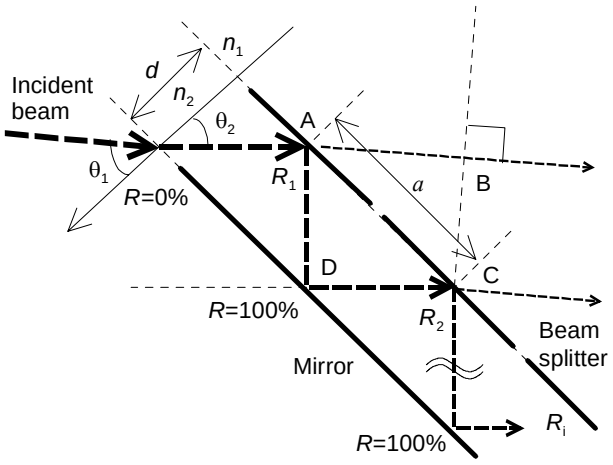

Figure 1. Beam splitting method to produce equal-intensity parallel beams. The device basically consists of a beam splitter and a mirror surface.

if we neglect any dispersion of n_1 and n_2. The OPD due to wavelength tuning between points B and C is

$$\Delta\Phi = \Delta\Phi_C - \Delta\Phi_B$$

$$= 2n_2 d\cos\theta_2\left(\frac{2\pi}{\lambda_1} - \frac{2\pi}{\lambda_0}\right), \tag{8}$$

if n_1=1.

C. Beam deflection

In the far field, this phase difference manifests itself as a deflection of the superimposed beams by an angle given as

$$\theta_{def} = \tan^{-1}\left[\frac{\left(\frac{\Delta\Phi}{k_1}\right)}{\overline{BC}}\right] = \tan^{-1}\left[\frac{\left(\frac{\lambda_1}{2\pi}\right)2n_2 d\cos\theta_2\left(\frac{2\pi}{\lambda_1} - \frac{2\pi}{\lambda_0}\right)}{a\cos\theta_1}\right], \tag{9}$$

where a is the aperture spacing of the beams on the beam splitter surface and $k_1 = 2\pi/\lambda_1$ is the wave number after wavelength tuning. The aperture spacing between two consecutive beams is given by $a = 2d\tan\theta_2$. Substituting $\theta_2 = \tan^{-1}(a/2d)$ into Eq. (9) and using the relation $n_1\sin\theta_1 = n_2\sin\theta_2$, the deflection angle follows as

$$\theta_{def} = \frac{n_2(2d/a)^2}{\sqrt{(2d/a)^2 + 1 - n_2^{\,2}}}\left(1 - \frac{\lambda_1}{\lambda_0}\right), \tag{10}$$

when the deflection angle is small, e.g. $\theta_{def} << \pi/2$. Defining a sensitivity coefficient

$$\alpha(a,d,n_2) = \frac{n_2(2d/a)^2}{\sqrt{(2d/a)^2 + 1 - n_2^{\,2}}}, \tag{11}$$

the deflection angle can be written as

$$\theta_{def} = \alpha(a,d,n_2)\left(1 - \frac{\lambda_1}{\lambda_0}\right). \tag{12}$$

D. Transmission efficiency

To obtain a feeling for the device loss we assume four beams (N = 4). The total output power from the MBG with four apertures is given by

$$\sum_{i=1}^{4} I_i = I(1-R_1) + IR_1R(1-R_2) + IR_1RR_2R(1-R_3) + IR_1RR_2RR_3R(1-R_4), \tag{13}$$

where I is the optical power of the input laser beam, I_i the optical power of the i-th output beam, and R the reflectance of the mirrored surface. Here we assume that there is neither a loss within the material nor one due to the partially reflecting coatings. The transmission efficiency of the MBG is then given by

$$\eta = \frac{\sum_{i=1}^{4} I_i}{I} = (1-R_1) + R_1 R\{(1-R_2) + R_2 R[(1-R_3) + R_3 R(1-R_4)]\}. \quad (14)$$

For a mirror coating with R=0.96 corresponding to the aluminum mirror at λ = 1.5 μm used for the experiments, the transmission efficiency is calculated to be -0.26 dB if the partial reflectivities R_i are chosen according to Eq. (1). With higher reflectance, a higher efficiency can be achieved (see Table 1).

Table 1. Transmission efficiencies of MBG for various mirror reflectances for a device generating four beams.

Reflectance on the mirror surface, R	Efficiency, η	
0.96	0.94	-0.26 dB
0.98	0.97	-0.13 dB
0.99	0.98	-0.07 dB

E. Two-dimensional beam scanning

To realize two-dimensional beam scanning, two MBGs are arranged orthogonally as shown in Fig. 2. The optical alignment for generating parallel beams is very simple even in the two-dimensional case. Each MBG has a different optical delay in order to produce different deflection sensitivities in vertical and horizontal direction. The deflection angles for the x and y directions are given by

$$\theta_x = \alpha_x \left(1 - \frac{\lambda_1}{\lambda_0}\right), \quad (15)$$

$$\theta_y = \alpha_y \left(1 - \frac{\lambda_1}{\lambda_0}\right), \quad (16)$$

where λ_0 and λ_1 are the wavelengths before and after wavelength tuning, respectively. One can show that the deflection sensitivity coefficients for the x and y directions are given by

$$\alpha_x = \frac{n_2 \gamma^2}{\sqrt{\gamma^2 + 1 - n_2^2}}, \quad (17)$$

$$\alpha_y = \frac{n_2 m^2 \gamma^2}{\sqrt{m^2 \gamma^2 + 1 - n_2^2}}, \quad (18)$$

where γ=($2d/a$) and the scaling factor m relates the thicknesses d' and d of the two MBG devices in the form $d' = md$. When the deflection sensitivity for the y axis becomes N times larger than that for the x axis,

$$\alpha_y = N\alpha_x, \quad (19)$$

the far-field optical beam can be steered within a square area across the receive plane (see Fig. 3) where N is the number of multiple beams for the x and y directions. Substituting Eqs. (17) and (18) into Eq. (19), we obtain the solution for the scaling factor m as

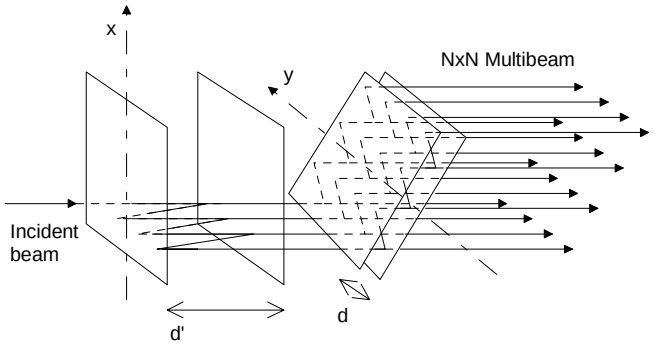

Figure 2. Method of generating two-dimensional multiple beams by introducing two relative optical time delays.

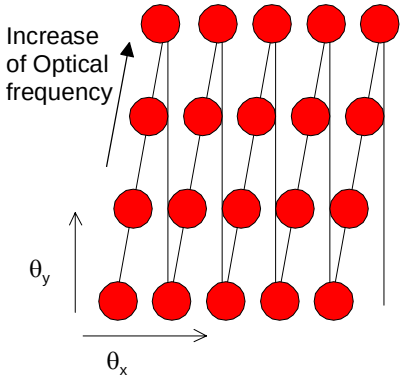

Figure 3. Explanation of two-dimensional raster beam scanning by wavelength tuning in the receive plane.

$$m = \sqrt{\frac{N^2\gamma^2 + \sqrt{N^4\gamma^4 + 4N^2\left(\gamma^2 + 1 - n_2^{\,2}\right)\left(1 - n_2^{\,2}\right)}}{2\left(\gamma^2 + 1 - n_2^{\,2}\right)}}\,. \tag{20}$$

When n_2=1, the scaling factor m equals N, that is $d' = Nd$.

F. Maximum deflection angle

The beam divergence of a coherent beam of diameter D is given by $\sim\lambda/D$. For a high filling factor, the beam divergence of an N-array beam becomes $\sim\lambda/(Na\cos\theta_1)$, where a is the aperture spacing of the beams. The side lobe is separated by $\lambda/(a\cos\theta_1)$ from the main lobe. Therefore, the maximum deflectable angle becomes $\pm\lambda/(2a\cos\theta_1)$, which is the range within the main lobe can be steered. The resolution of beam scanning along one axis can be equal to the diffracted beam width of $\lambda/(Na\cos\theta_1)$ when the condition in Eq. (20) is maintained, which is the same divergence angle of the beam. A more precise resolution of beam scanning can be realized for the raster scan if the thickness of the MBG for the y-axis deflection is larger than Nd.

III. Experimental setup and results

A. One-dimensional beam scanning

An MBG with a thickness of $d = 2$ mm was manufactured. As shown in Fig. 4, the design was slightly modified compared to that presented in Fig. 1. With the exception of the first partially reflecting surface, the reflectance of the coatings was designed according to Eq. (1). The actual data are presented in Table 2. A photo of the MBG is shown in Fig. 5.

Table 2. Reflectance of the manufactured MBG.

Reflectance	designed	actual
1st coating, R_1	25 %	25 %
2nd coating, R_2	66.7 %	66 %
3rd coating, R_3	50 %	49.5 %
4th coating, R_4	0 %	0.85 %
Mirror coating, R	100 %	96 %

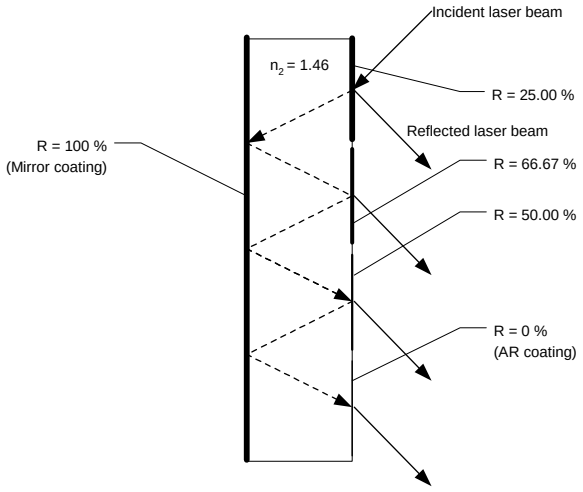

Figure 4. Design of an optical delay device with four beam output apertures.

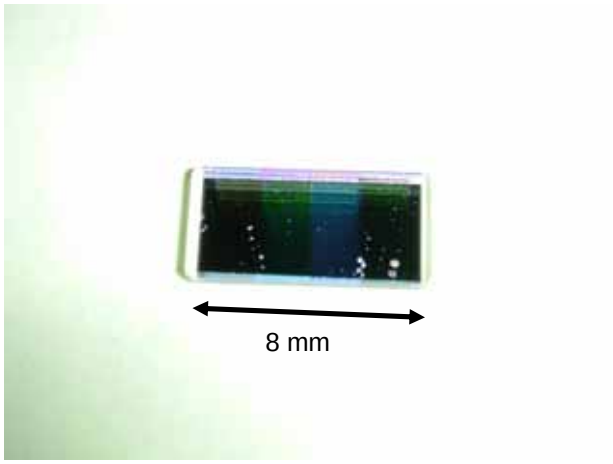

Figure 5. Photograph of the manufactured optical delay device with four beam output apertures.

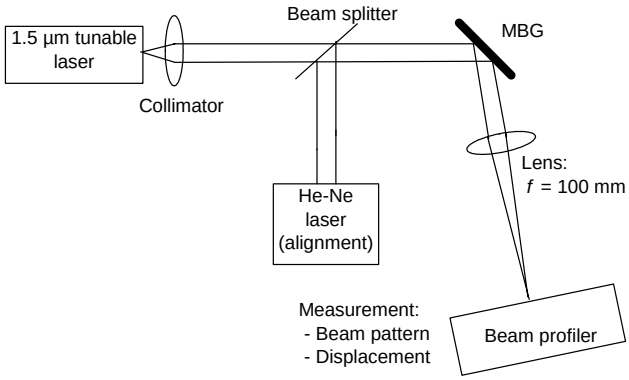

Figure 6. Experimental setup for the beam deflection measurement.

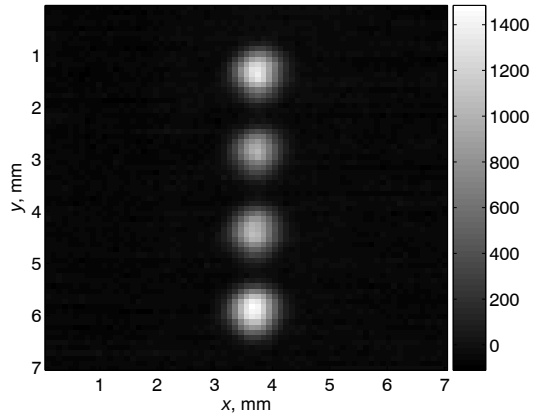

Figure 7. Intensity distribution of the 1 × 4 beam array just behind the MBG.

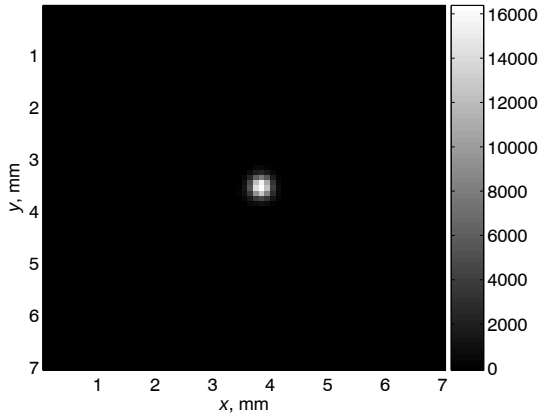

Figure 8. Far field pattern of the 1 × 4 beam array as obtained in the focal plane of a lens.

Using a wavelength of 1550 nm, the optical beam pattern was measured using the configuration of Fig. 6. The 1 × 4 laser beam intensity distribution just behind the MBG is shown in Fig. 7. Each beam has almost the same intensity distribution, as designed. The 1 × 4 laser beam array was then focused with a lens, with the intensity distribution obtained as shown in Fig. 8. For the following beam deflection measurement, only two laser beams were used; otherwise, the low resolution of the beam profiler available (i.e. 1 mrad) would not have been sufficient. (With a smaller total aperture, the deflection angle will be larger.) The deflection characteristics of the peak intensity as a function of the optical wavelength are shown in Fig. 9. The maximum beam deflection angle was calculated to be ±517 μrad in this case.

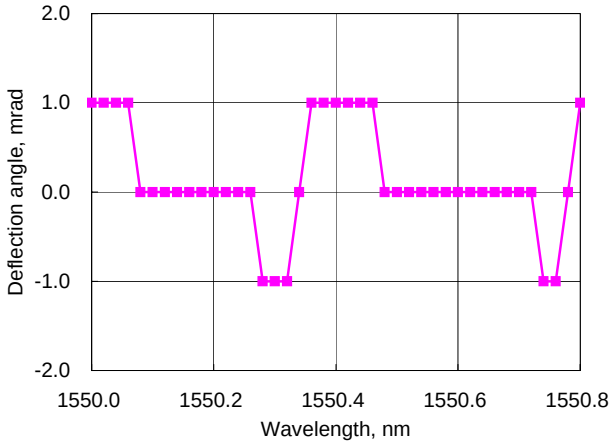

Figure 9. One-dimensional deflection characteristic of the 1 × 2 beam array as a function of wavelength. (Because of the low resolution of the measurement setup of 1 mrad, the discrete 3-level result was to be expected.)

B. Two-dimensional beam scanning

Two MBGs, one 2-mm thick and the other1 mm, were set up as shown in Fig. 10 for two-dimensional beam scanning. The first MBG generated two output beams; the second one was arranged normally and doubled the number of input beams. Thus, the output was a 2 × 2 beam array.

With the configuration shown in Fig. 10 the optical beam pattern was measured (see Fig. 11). The beams differ in intensity because the incident angle was set to 45 deg in spite of the design value of 40.8 deg to arrive at an easier layout for the optical elements.

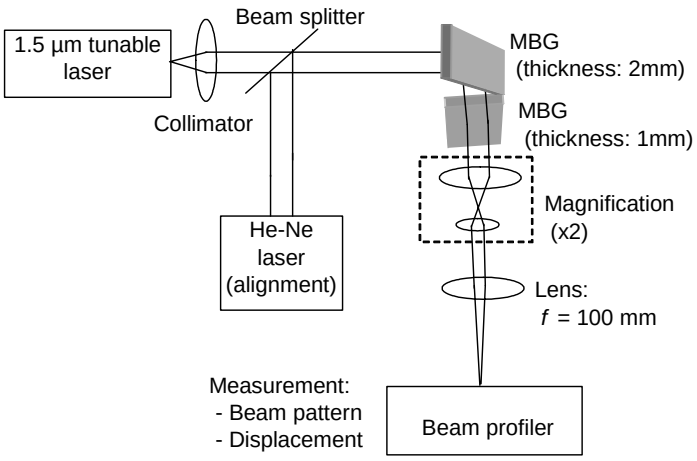

Figure 10. Experimental setup for the beam deflection measurement.

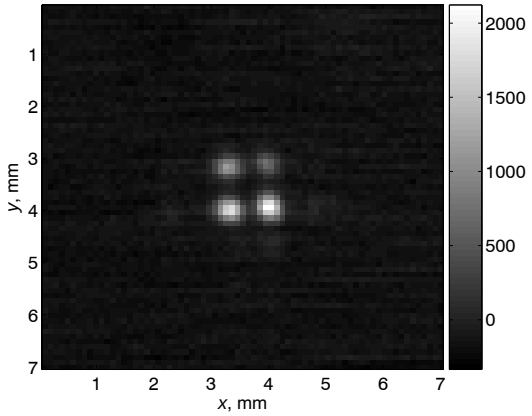

Figure 11. Intensity distribution of the 2 × 2 beam array just behind the second MBG (see Fig. 10).

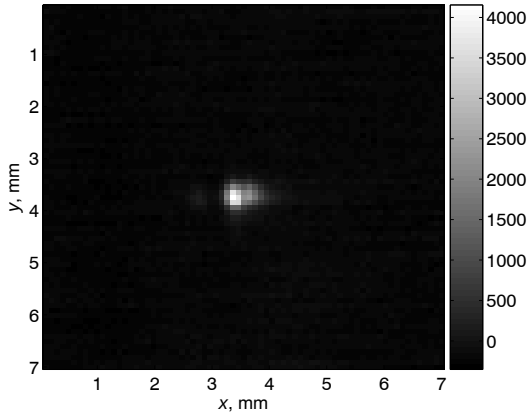

Figure 12. Far field pattern of the 2 × 2 beam array as obtained in the focal plane of a lens (see Fig. 10).

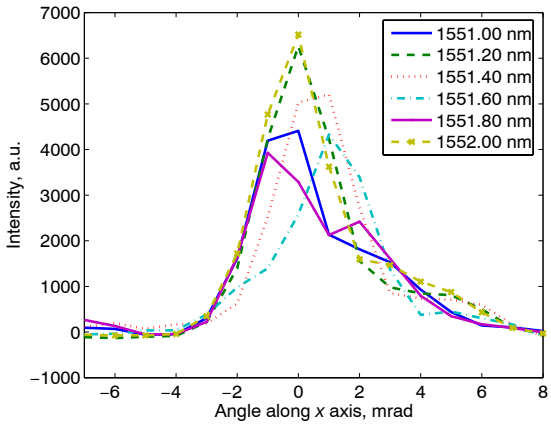

Figure 13 (a). Beam patterns along the x axis as a function of wavelength.

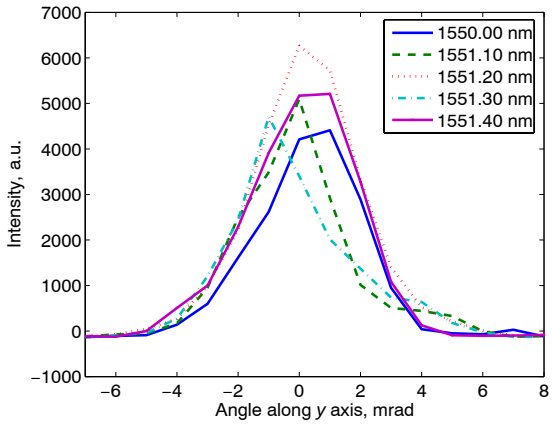

Figure 13(b). Beam patterns along the *y* axis as a function of wavelength.

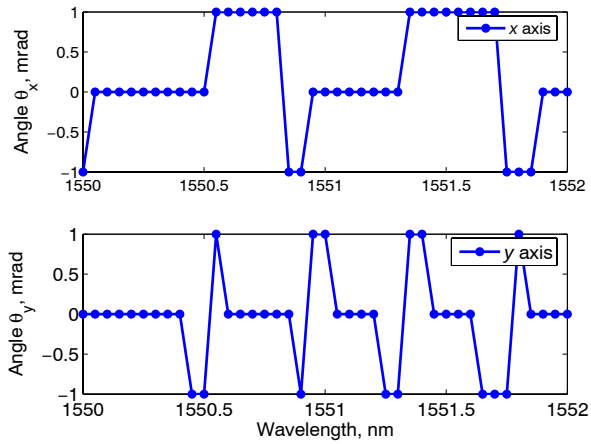

Figure 14. Two-dimensional deflection characteristics of the 2 × 2 laser beams.

The 2 × 2 laser beam array was focused with a lens and the intensity distribution was measured. Figure 12 shows the focused image of the array at a wavelength of 1550 nm. Figures 13(a) and (b) show the beam pattern for x and y axes as a function of wavelength, demonstrating that the peak intensity is steered. The two-dimensional deflection characteristics as a function of the optical wavelength are shown in Fig. 14. The direction of the peak intensity is plotted as a function of the wavelength. The deflection characteristic along the y axis with (MBG with 2-mm thickness) shows higher deflection sensitivity against the wavelength than that along the x axis (MBG with the 1-mm thickness). As the sensitivity coefficients are different for orthogonal directions, a two-dimensional raster scan is achieved.

IV. Influence of phase error

A. Measurement of optical phase

The concept proposed works only for well-defined phase differences between the individual beams of the array. Only if the phase differences are equal, with a value dependent just on the wavelength, will the beam deflection as described in the previous sections result in the far field. We have analyzed the influence of the phase error on the intensity of the beam in the far field. For the analysis, we assumed four circular apertures with the uniform intensity distribution as shown in Fig. 15. In the far field the optical intensity is given by the two-dimensional Fourier transform. Figs. 16(a) and (b) show examples of the far-field intensity with and without a random phase error among the optical beams. In the presence of a phase error, the on-axis optical power is reduced and spread into other directions.

We have calculated the normalized peak intensity and plotted it as a function of the rms piston phase error in Fig. 17. The phase error must correspond to less than $\lambda/10$ rms in order to maintain the coherent combining effect.

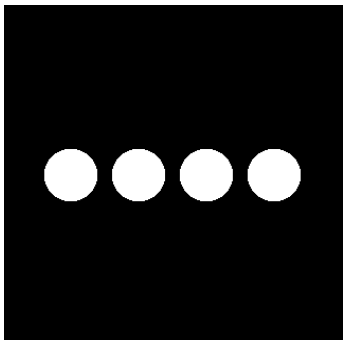

Figure 15. Aperture function of the beams.

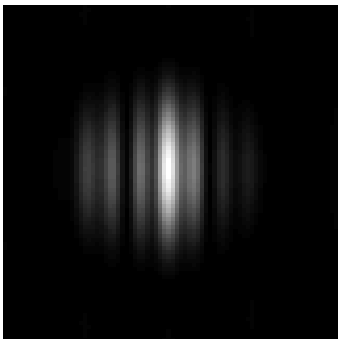

Figure 16(a). Simulated optical intensity with random piston phase error.

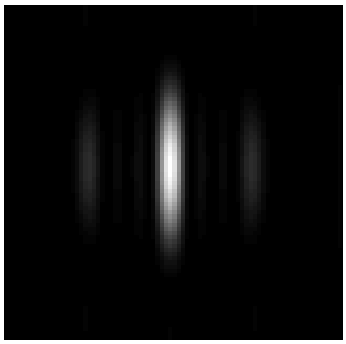

Figure 16(b). Simulated optical intensity without random piston phase error.

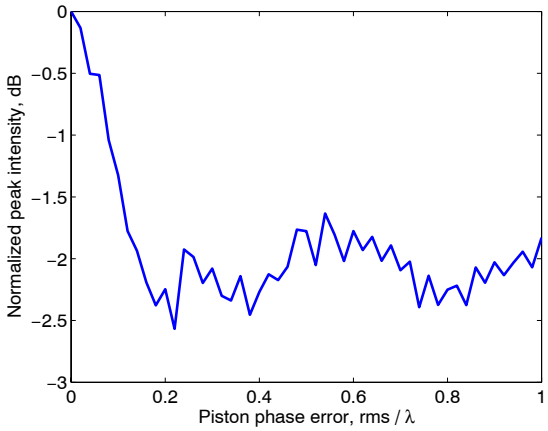

Figure 17. Degradation of the far-field on-axis intensity due to the random piston phase error in the 1 × 4 laser beam array.

B. Measurement of optical phase

To measure the phase difference between the four beams of a 1 × 4 beam array, an interferometer as shown in Fig. 18 was set up. The beams produced by the MBG [Fig. 19(a)] are superimposed by a broad beam derived from the same source [Fig. 19(b)], resulting in an interference pattern which was recorded by the beam profiler [Fig. 19(c)]. (The intensities of the beams are not equal because the 1-mm-thick MBG was used with a larger incident angle than the designed value.) Any phase difference between the four beams would manifest itself in fringe patterns shifted relative to each other. If there is no phase error among the beams, the interference maxima (and minima) will occur along a straight line. This can be seen to be the case in Fig. 19(c) which indicates that the partially reflective coatings deposited on the MBG had negligible influence on the phase shift difference of the transmitted laser beams.

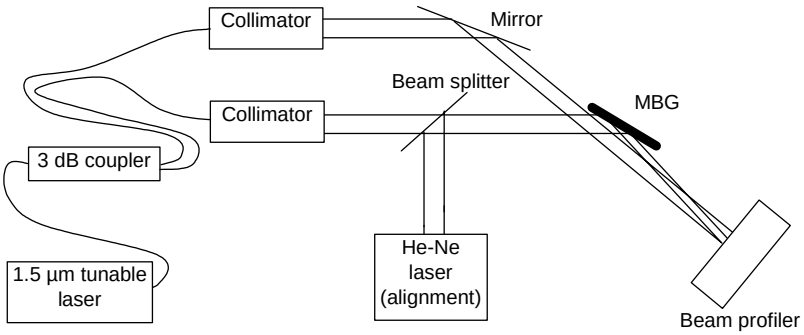

Figure 18. Experimental setup for the fringe measurement.

V. Conclusion

A two-dimensional raster beam scanning method effectuated by only wavelength tuning was proposed. Devices with an optical delay line structure were manufactured and the beam deflection performance was tested. The principle for the two-dimensional beam deflection was experimentally confirmed. The speed of beam deflection is limited by the rate of wavelength tuning of the laser source or optical modulator involved. However, the rise and fall times of the optical signal are affected by the delay time within the array. The proposed method offers a very simple optical phased array concept and can be used for future free-space multicast optical communications in terrestrial and space applications.

References

[1]P. F. Mcmanamon, T. A. Dorschner, D. L. Corkum, L. J. Friedman, D. S. Hobbs, M. Holz, S. Liberman, H. Q. Nguyen, D. P. Resler, R. C. Sharp, and E. A. Watson, "Optical phased array technology," *Proceeding of IEEE*, Vol. 84, No. 2, 1996, pp. 268-298.

[2]K. H. Kudielka, A. Kalmar, W. R. Leeb, "Design and breadboarding of a phased telescope array for free-space laser communications," Proceeding of IEEE International Symposium on Phased Array Systems and Technology, 1996, pp. 419-424.

[3]D. Bushuev, D. Kedar, S. Arnon, "Analyzing the performance of a nanosatellite cluster-detector array receiver for laser communication," *Journal of Lightwave Technology*, Vol. 21, No.2, 2003, pp. 447-455.

[4]A. Polishuk, and S. Arnon, "Communication performance analysis of microsatellites using an optical phased array antenna," *Optical Engineering*, Vol. 42, No.7, 2003, pp. 2015-2024.

[5]H. S. Hinton, "Photonic switching fabrics," *IEEE Communications Magazine*, Vol. 28, No. 4, April 1990, pp. 71-89.

[6]M. Yamaguchi, T. Yamamoto, K. Hirabayashi, S. Matsuo, K. Koyabu, "High-density digital free-space photonic-switching fabrics using exciton absorption reflection-switch (EARS) arrays and microbeam optical interconnections," *IEEE Journal of Selected Topics in Quantum Electronics*, Vol. 2, No. 1, 1996, pp. 47- 54.

[7]T. Yamamoto, M. Yamaguchi, K. Hirabayashi, S. Matsuo, C. Amano, H. Iwamura, Y. Kohama, T. Kurokawa, K. Koyabu, "High-density digital free-space photonic switches using micro-beam optical interconnections," *IEEE Photonics Technology Letters*, Vol. 8, No. 3, 1996, pp. 358-360.

[8]J.-P. Herriau, A. Delboulbe, J.-P. Huignard, G. Roosen, G. Pauliat, "Optical-beam steering for fiber array using dynamic holography," *Journal of Lightwave Technology*, Vol. 4, No. 7, 1986, pp. 905-907.

[9]B. Winker, M. Mahajan, M. Hunwardsen, "Liquid crystal beam directors for airborne free-space optical communications," *IEEE Aerospace Conference Proceedings*, Vol. 3, March 2004, pp. 6-13.

[10]Y. Murakami, K. Inagaki, Y. Karasawa, "Beam forming characteristics of a waveguide-type optical phased array antenna," *IEICE Transaction of Communication*, Vol. E80-B, No.4, 1997.

[11]K. Inagaki and Y. Karasawa, "Three-element fiber-type optical phased array antenna with high-speed two-dimensional optical beam steering," *Electron. Commun. Jpn.*, Vol. 82, 1999, pp. 42-51.

[12]T. Kawanishi, K. Higuma, T. Fujita, J. Ichikawa, T. Sakamoto, S. Shinada, M. Izutsu, "$LiNbO_3$ high-speed optical FSK modulator," *Electronics Letters*, Vol. 40, No. 11, 2004, pp. 691-692.

[13]T. Kawanishi, K. Higuma, T. Fujita, J. Ichikawa, T. Sakamoto, S. Shinada, M. Izutsu, "High-speed optical FSK modulator for optical packet labeling," *Journal of Lightwave Technology*, Vol. 23, No.1, 2005, pp.87-94.

[14]M. Toyoshima and K. Araki, Japan Patent Application for a "Beam splitting method," No. 3069703, filed 24 Nov. 1999.

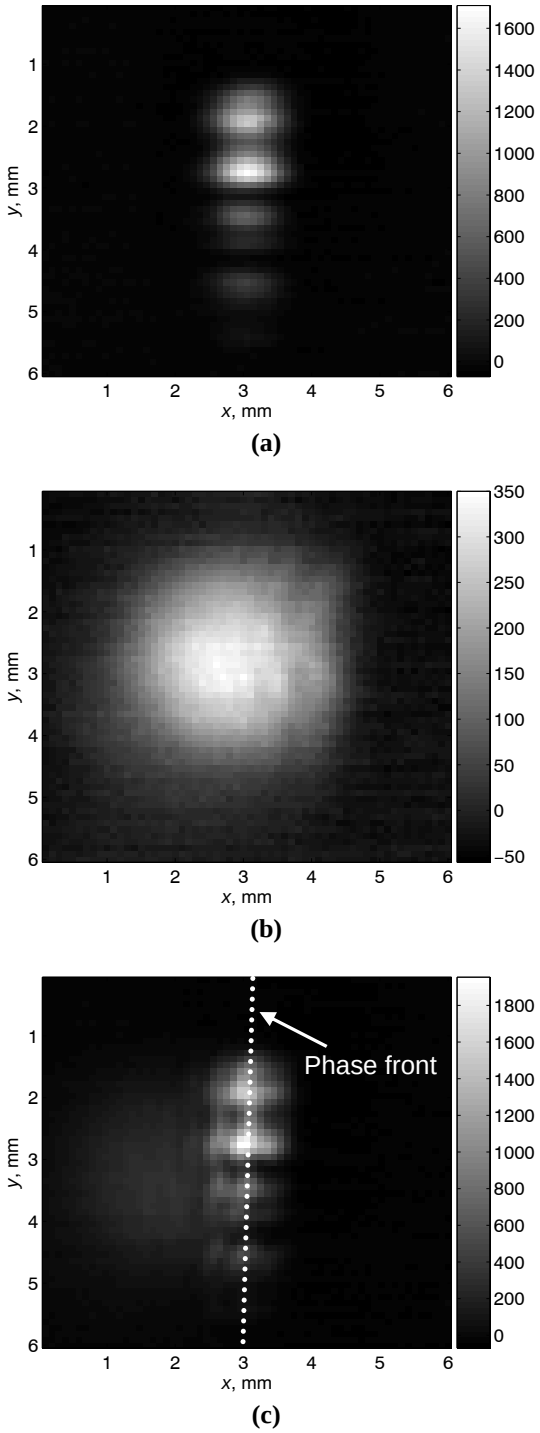

Figure 19. Intensity distributions of (a) 1 × 4 array beam, (b) local beam and (c) interference pattern.